Is a position-dependent stiffness relevant for the wetting phase diagram?

F. Clarysse and C. J. Boulter
Department of Mathematics, Heriot-Watt University, Edinburgh EH14 4AS, United Kingdom
(Received 8 October 2001; published 27 February 2002)

In this paper we determine the wetting phase diagram for three-dimensional systems with short-range forces assuming the presence of a position-dependent stiffness contribution as recently proposed [M.E. Fisher and A.J. Jin, Phys. Rev. Lett. **69**, 792 (1992)]. We predict a discontinuous transformation of the phase diagram immediately upon moving beyond the mean-field approximation. However, in contrast to Fisher and Jin we find that a renormalization group calculation yields fluctuation-induced second-order transitions rather than fluctuation-induced first-order ones. As a consequence, in all fluctuation regimes we recover the same qualitative phase diagram as predicted in the absence of a position-dependent stiffness coefficient. Furthermore, recent predictions for tricritical wetting behavior remain unaffected by the stiffness contribution.

DOI: 10.1103/PhysRevE.65.031607 PACS number(s): 68.08.Bc, 64.60.Fr, 68.35.Rh, 05.70.Fh

I. INTRODUCTION

There has been considerable controversy over recent years concerning wetting behavior in systems with short-ranged forces at the upper critical dimension $d=3$ (see [1–3] and references therein). One of the most intriguing predictions in this area was made by Fisher and Jin (FJ) [4] who suggested that mean-field critical wetting transitions may be driven first order due to fluctuation effects. This prediction stems from an alteration in the interface model used in the fluctuation studies.

In this paper we revisit the FJ model and examine the entire phase diagram, not just the region corresponding to mean-field critical wetting transitions. In this way we observe that the most dramatic modification to the phase diagram is not genuinely caused by fluctuation effects but occurs discontinuously as soon as one proceeds beyond the mean-field approximation. This change is due to a switch in sign of the next-to-leading order term in the appropriate effective interface potential. A detailed linear renormalization group study is performed to determine fluctuation effects and the resulting phase diagrams are compared with those found from a traditional capillary wave model [5]. Topologically the two cases are qualitatively the same with the phase diagrams simply a mirror image of one another. As a result we predict that one observes first-order wetting transitions becoming fluctuation induced second order, in contrast to the FJ scenario described above. We stress that these differences do not reflect an error in the FJ analysis. Rather, we agree with the calculation of FJ but extend their study leading to a reinterpretation of the results.

The remainder of the paper is arranged as follows. In the next section we review the pertinent details of wetting behavior predicted from the capillary wave model and describe the FJ model. In Sec. III we perform a detailed analysis of the phase behavior predicted from the FJ model and contrast this with results of the capillary wave model. Finally, in Sec. IV we discuss the main results and present our conclusions.

II. BACKGROUND

In what follows we consider a semi-infinite system with a two-dimensional planar surface in the plane $z=0$. We assume that a phase α is preferentially adsorbed at the surface, while a second phase β is stable in the bulk, i.e., infinitely far from the surface. The location of the interface between the two phases is denoted by l so that $\langle l\rangle$ represents the average thickness of the adsorbed layer. The wetting transition corresponds to a divergence of $\langle l\rangle$ as an external field such as the temperature is varied. This surface phase transition may be either first or second order (critical).

A. Capillary wave model

One of the most profitable methods of studying wetting behavior is via the introduction of an effective interface model which is a functional of the layer thickness l. Traditionally this takes the form [6]

$$H_I[l]=\int d\mathbf{y}\left\{\frac{1}{2}\Sigma_{\alpha\beta}(\nabla l)^2+W(l;T,\ldots)\right\}, \qquad (1)$$

and is known as the capillary wave model. Here $\mathbf{y}$ denotes the vector displacement along the fixed surface and $\Sigma_{\alpha\beta}$ is the surface tension of the α-β interface. The interaction between the surface and the interface is described by the binding potential $W(l)$, the shape of which fully determines the phase behavior at mean-field (MF) level. In this paper we are interested only in systems with short-ranged forces for which $W(l)$ is given by the expansion [6,7]

$$W(l)=ae^{-\kappa l}+be^{-2\kappa l}+ce^{-3\kappa l}+\cdots, \qquad (2)$$

for $l>0$, assuming bulk two-phase coexistence. The coefficient a takes the form $a\propto(T-T_W^{\mathrm{MF}})$ where T_W^{MF} is the mean-field critical wetting temperature, while the coefficient c is assumed to be a strictly positive constant so that we can truncate the expansion after three terms. Finally, $\kappa=1/\xi_b$ is the inverse bulk correlation length of the wetting (α) phase.

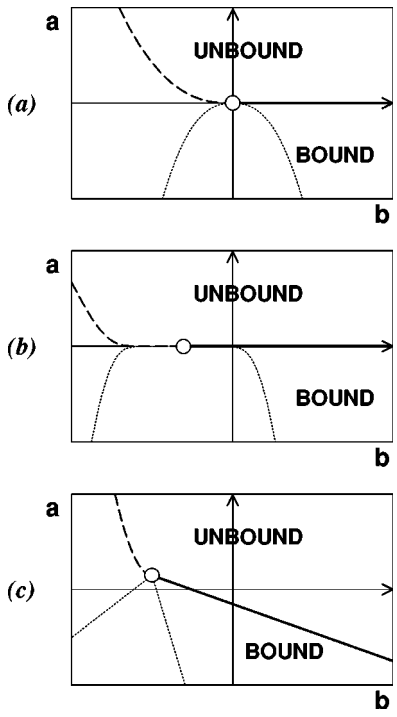

FIG. 1. Schematic representation of the renormalized (a-b) phase diagram obtained from the capillary wave model (1) for the different fluctuation regimes. Critical wetting phase boundaries are shown by thick solid lines, first-order phase boundaries by dashed lines, and the locus of tricritical behavior by dotted lines. In each case, the tricritical point is indicated by an open circle. (a) corresponds to all regimes with $\omega<1/2$, (b) corresponds to $1/2<\omega<2$, while (c) represents the case $\omega>2$.

At the mean-field level one simply ignores fluctuations of the interface and hence the phase diagram follows from minimizing Eq. (2). To determine the effect of fluctuations, on the other hand, one needs to perform a renormalization group (RG) analysis of the interface model (1). Application of an exact linear RG predicts the existence of at least three distinct regimes parametrized by the dimensionless capillary parameter [6–8]

$$\omega=\frac{k_B T_W}{4\pi\Sigma_{\alpha\beta}\xi_b^2}. \tag{3}$$

We note here that the limit $\omega\to 0^+$ is expected to yield MF predictions since it corresponds to a nonfluctuating interface with $\Sigma_{\alpha\beta}\to\infty$. The full linear RG study of the model (1) with the potential (2) is reported in Ref. [5] and it is appropriate to recall here the main results which are best summarized by referring to Fig. 1. This is a schematic representation of the renormalized (a-b) phase diagram for three fluctuation regimes. In each of the regimes, critical phase boundaries are shown by thick solid lines, first-order phase boundaries by dashed lines, and the locus of tricritical-like behavior by dotted lines. Focusing first on the critical transition we observe that in regimes I and II (with $\omega<1/2$ and $1/2<\omega<2$, denoted the weak and intermediate fluctuation regimes, respectively [9]) the wetting temperature is at $a=a_c=0$ as in the mean-field case, while in regime III ($\omega>2$, strong fluctuation regime) the transition temperature is generally reduced [8]. The predictions for the critical behavior are strongly nonuniversal such that, for example, the correlation length parallel to the interface, $\xi_\parallel$, diverges on approach to the wetting temperature according to $\xi_\parallel\sim(T_W-T)^{-\nu_\parallel}$ where

$$\nu_\parallel=\begin{cases}1/(1-\omega), & \omega<1/2,\\ 1/(\sqrt{2}-\sqrt{\omega})^2, & 1/2<\omega<2,\\ \infty, & \omega>2,\end{cases} \tag{4}$$

and where the result for $\omega>2$ corresponds to an exponential divergence of $\xi_\parallel$ [8].

As regards the first-order scenario the RG analysis is a little more involved as in principle four, rather than three, distinct regimes are found [5]. However, the behavior in the first two regimes (corresponding to $\omega<2/9$ and $2/9<\omega<1/2$) is qualitatively identical. In particular, the tricritical point remains at its MF value $b=b_t=0$ and the first-order phase boundary for small b is described by the power law

$$a\sim b^{\psi}, \tag{5}$$

where the exponent ψ is given by [5]

$$\psi=\begin{cases}(2-3\omega)/(1-3\omega), & \omega<2/9,\\ (\sqrt{2}-\sqrt{\omega})^2/(\sqrt{2}-2\sqrt{\omega})^2, & 2/9<\omega<1/2.\end{cases} \tag{6}$$

For $1/2<\omega<2$ the tricritical point is shifted to $b=b_t<0$ with a critical transition for $b>b_t$ and a first-order transition for $b<b_t$. Note that this point still occurs at the MF wetting temperature $a=0$. In this regime the phase boundary is described by $a\sim(b_t-b)^{\psi}$ where the exponent $\psi=\infty$ indicates an exponential, rather than algebraic, path. Finally, a fourth regime applies for $\omega>2$ with the tricritical point shifted to $b_t<0$ and $a>0$.

Tricritical points generally lie in a different universality class from the second-order transition and so one expects different critical exponents. Renormalization group calculations reveal that this is true only for $\omega<1/2$. More specifically, for the tricritical wetting transition, three fluctuation regimes are again found but Eq. (4) is replaced by [5,10,11]

$$\nu_\parallel=\begin{cases}3/(4-6\omega), & \omega<2/9,\\ 1/(\sqrt{2}-\sqrt{\omega})^2, & 2/9<\omega<2,\\ \infty, & \omega>2.\end{cases} \tag{7}$$

The boundary of the region in the phase diagram in which this tricritical-like behavior will be observed is denoted by the dotted lines in Fig. 1.

It is appropriate to confirm at this stage that the mean-field phase diagram is qualitatively identical to the phase diagram in the first regime [Fig. 1(a)]. Moreover, quantitatively, all the MF results are recovered in the limit $\omega\to 0^+$. To understand the effect of fluctuations one should compare

the phase behavior in this limit to the results for strictly positive ω. From Fig. 1 it is then clear that the shift of the tricritical point for $\omega > 1/2$ means that first-order wetting transitions can be driven *fluctuation induced second order*.

B. Fisher-Jin model

The capillary wave model (1) and (2) may be justified phenomenologically; however, a recent study by Fisher and Jin has shown that it does not withstand a more rigorous examination [4,12,13]. In particular, FJ derive an interface model from the underlying microscopic Landau-Ginzburg theory by introducing an appropriate definition of the collective coordinate l and applying a saddle-point approximation in the corresponding minimization procedure. In so doing they find a revised model of the form

$$H_I[l] = \int d\mathbf{y} \left\{ \frac{1}{2}\Sigma(l)(\nabla l)^2 + W_{\mathrm{FJ}}(l;T,\ldots) \right\}, \qquad (8)$$

with, most importantly, the presence of a position-dependent stiffness coefficient $\Sigma(l) = \Sigma_{\alpha\beta} + \Delta\Sigma(l)$. To leading order the position-dependent contribution is $\Delta\Sigma(l) = -q\kappa l e^{-2\kappa l} + \cdots$. Furthermore, FJ also predict that in addition to the terms in Eq. (2) there are nonpure exponential contributions in the expansion for the binding potential $W_{\mathrm{FJ}}(l)$, although their coefficients vanish at T_W^{MF}. To highlight the effect of these modifications on the RG analysis, we recall here some of the pertinent details of the linear RG scheme.

For the capillary wave model (i.e., in the absence of a position-dependent stiffness coefficient) Fisher and Huse [8] showed that the binding potential is renormalized according to

$$W^{(t)}(l) = \frac{e^{2t}}{\sqrt{4\pi\omega t}} \int_{-\infty}^{\infty} dl' W^{(0)}(l') e^{-(l-l')^2/4\omega t}, \qquad (9)$$

where t is the renormalization parameter and $W^{(0)}(l)$ is the initial bare potential given (for $l > 0$) by Eq. (2). Formally, one should include a hard wall such that W is infinite for $l < 0$ since the α-β interface cannot pass through the wall. However, a potential that diverges cannot be handled by a linearized RG and so instead we settle for the soft-wall restriction $W^{(0)}(l) = w_0 > 0$ for $l < 0$ [14]. In the case of the FJ model the linear RG analysis is more complicated due to a coupling between the RG flows of $\Delta\Sigma^{(t)}(l)$ and $W_{\mathrm{FJ}}^{(t)}(l)$. Surprisingly, the results of the procedure can be written in a simple form. In particular, one finds that the binding potential renormalizes exactly as in the standard case, i.e., according to Eq. (9), except with the initial bare potential $W^{(0)}(l)$ replaced by the modified expression

$$\tilde{W}^{(0)}(l) = W_{\mathrm{FJ}}^{(0)}(l) + \frac{\omega\xi_b^2\Lambda^2}{2}(1 - e^{-2t})\Delta\Sigma^{(0)}(l), \qquad (10)$$

where Λ is the momentum cutoff implicitly assumed within the interface models. For large t Eq. (10) simply amounts to changing $W_{\mathrm{FJ}}^{(0)}$ by a term proportional to $\Delta\Sigma^{(0)}$ and thus the dominant terms in $\Delta\Sigma^{(0)}(l)$ can compete with terms in the initial potential $W_{\mathrm{FJ}}^{(0)}(l)$. More specifically, with $\Delta\Sigma$ of the form described above, the contribution $-q\kappa l e^{-2\kappa l}$ becomes the subdominant one in the modified potential (10). As a result, FJ concluded that for $q > 0$ this effect may serve as a destabilizing mechanism for the bare critical transition, observing first-order transitions in regions in which the MF analysis predicts critical transitions. However, the analysis was restricted to the case of a fixed positive b value and thus their results cannot be conclusive about the net effect of the position-dependent stiffness coefficient on the full (a-b) phase diagram.

In the next section we carefully reanalyze the FJ model to understand the influence of this revised subdominant term in the modified potential on the renormalized phase diagrams of Fig. 1. Moreover, while neglected in the FJ study, we do incorporate the explicit b dependence of the coefficient q. Indeed, explicit calculations reveal quite generally that q is proportional to b with both coefficients changing sign at the mean-field tricritical point. In particular, $q = \omega(\xi_b\Lambda)^2 b$. Estimates by Evans, Hoyle, and Parry [15] for the true bulk correlation length indicate that $\xi_b^2\Lambda^2$ is of order 1 for relevant temperatures and hence we assume $q \approx \omega b$ for our study, although our results remain valid for $q = \eta\omega b$ with any constant of proportionality η.

III. PHASE DIAGRAM FOR THE FISHER-JIN MODEL

From here on we assume that lengths are measured in units of ξ_b so the modified potential (10) can be expanded as

$$\tilde{W}^{(0)}(l) = ae^{-l} + b(1 - \omega l)e^{-2l} + ce^{-3l} + \cdots. \qquad (11)$$

Before performing the integration in Eq. (9) associated with the full RG analysis, it is instructive to first gauge the effect of the additional term by examining the modified potential in a mean-field-like way for (small) fixed ω, i.e., we determine the phase diagram by minimizing Eq. (11). The same qualitative behavior is then expected in the weak fluctuation regime of the RG so that this analysis provides helpful insight into the renormalized phase diagram.

Obviously, in comparison to the standard potential (2), the stiffness contribution changes the sign of the next-to-leading order term; therefore significant modifications in the phase behavior are anticipated. As depicted in Fig. 2 where we compare the MF phase diagrams corresponding to Eqs. (2) and (11), we find that for arbitrarily small positive ω the critical transition for $b > 0$ vanishes and is replaced by a first-order wetting transition. Generally this phase boundary is linear as described by

$$a \sim e^{-(1+\omega)/\omega}\omega b. \qquad (12)$$

The presence of the exponential factor indicates that for small ω the phase boundary lies extremely close to the b axis. Formally Eq. (12) is valid in the limit of large b, but it appears to be in good agreement with numerical solutions whenever $b \gtrsim 1$. In the limit of $b \to 0+$ the phase boundary is given by $a \sim \omega b^2 \ln(1/b)$. For $b < 0$ the next-to-leading order term in $\tilde{W}^{(0)}(l)$ is positive and a window of critical wetting

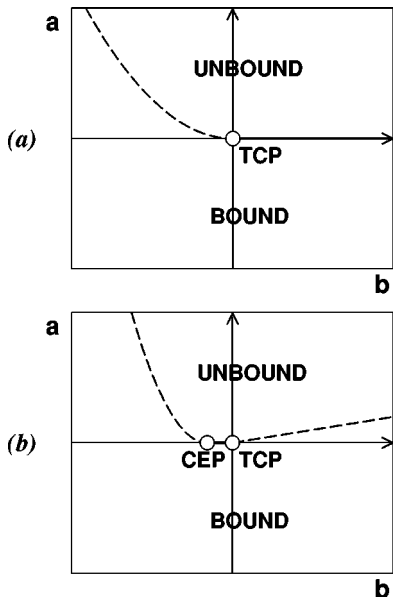

FIG. 2. Mean-field (a-b) phase diagrams for (a) the standard potential (2), and (b) the modified potential (11). Critical phase boundaries are given by the thick solid lines, while dashed lines show first-order phase boundaries.

transitions is found on the $a=0$ axis. The critical and first-order phase boundaries join smoothly at a tricritical point located at $a=b=0$. For larger negative values of b the critical phase boundary terminates at a critical end point, the location of which is given by

$$|b_{\mathrm{CEP}}| = \frac{c}{\omega} e^{-(1-\omega)/\omega}, \tag{13}$$

where here the exponential factor reveals that the width of the critical region is small for small ω. This critical end point is also the terminus of a further first-order phase boundary. It is crucial to stress at this stage that the presence of both the critical end point and the connected first-order phase boundary is purely artificial. Specifically, they originate from the truncation of the expansion for the binding potential which leads to an unphysical, finite potential at $l=0$. As a result one can create an unphysical minimum at small finite l (in some cases a boundary minimum). In reality the binding potential should satisfy $W(l\to 0+)\to\infty$ so that such minima cannot lead to extra phase transitions. The irrelevance of this feature in our model is further confirmed by the observation that, by increasing the value of the positive coefficient c [and hence $W(l=0)$], the critical region increases in size. Moreover, as demonstrated below, this artifact is removed entirely by the RG procedure in stronger fluctuation regimes.

From the above discussion we predict a dramatic modification to the phase diagram as soon as one switches on the fluctuations (i.e., as soon as we allow a nonzero ω, however small). The genuine MF behavior is recovered when $\omega=0$ and is, by construction, identical to that found from the capillary wave model shown in Fig. 2(a). Crucially this behavior is different from that found in the limit of $\omega\to 0+$ embodied in Fig. 2(b). Hence we propose that the inclusion of the position-dependent stiffness leads to a discontinuous change of the phase diagram immediately upon proceeding beyond mean-field level. We reiterate that this is entirely due to a switch in sign of the next-to-leading order term in the binding potential. The genuine effects of the fluctuations, however, become apparent only upon performing the appropriate RG analysis and comparing the results to the phase diagram given in Fig. 2(b). The remainder of this section is devoted to precisely this task.

As discussed by Fisher and Huse [8], when using the linearized RG to study wetting phenomena, a matching procedure must be employed since there is no nontrivial fixed point representing the wetting transition. In practice, this implies that we renormalize to a scale $t^{\dagger}$ at which the curvature of $W^{(t)}(l)$ at the minimum is of order 1 and increasing; at this point one may expand the potential around the minimum and use mean-field theory to determine the critical behavior (further details can be found in [2,8,5]). Within the linear RG theory one may renormalize each term in the bare potential individually and simply sum up the results to obtain $W^{(t)}(l)$. To this end we note that if $V^{(0)}(l)=e^{-nl}$ for $l>0$ and $V^{(0)}(l)=0$ for $l<0$ then, using the method of steepest descent, one finds

$$V^{(t)}(l)\approx\begin{cases} e^{-nl+(2+n^2\omega)t}, & l>2n\omega t, \\ \dfrac{1}{\sqrt{4\pi\omega t}}\dfrac{1}{(n-l/\omega t)}e^{2t-l^2/4\omega t}, & l<2n\omega t. \end{cases} \tag{14}$$

Similarly, if $V^{(0)}(l)=le^{-2l}$ for $l>0$ and vanishes for $l<0$, the renormalization yields

$$V^{(t)}(l)\approx\begin{cases} (l-4\omega t)e^{-2l+(2+4\omega)t}, & l>4\omega t, \\ \dfrac{1}{\sqrt{4\pi\omega t}}\dfrac{1}{(2-l/\omega t)^2}e^{2t-l^2/4\omega t}, & l<4\omega t, \end{cases} \tag{15}$$

while the soft-wall contribution renormalizes to $2\omega t w_0 e^{2t-l^2/4\omega t}/(l\sqrt{4\pi\omega t})$ for all $l>0$ [8,13]. With these results we immediately identify four distinct regimes associated with $l>6\omega t$, $6\omega t>l>4\omega t$, $4\omega t>l>2\omega t$, and $l<2\omega t$. However, as shown below, we find that the behavior in the first two regimes is qualitatively identical.

The first regime has $l>6\omega t$ which may be identified *a posteriori* with $\omega<2/9$, and thus from above the renormalized potential reads

$$W^{(t)}(l)\approx ae^{-l+(2+\omega)t}+b[1-\omega(l-4\omega t)]e^{-2l+(2+4\omega)t} + ce^{-3l+(2+9\omega)t}. \tag{16}$$

Applying the RG matching procedure results in the phase diagram depicted in Fig. 3(a). Note the resemblance to Fig. 2(b). For the critical and tricritical behavior we recover the standard results as given in Eqs. (4) and (7), respectively. For $b>0$ the wetting transition is always found to be of first order. Near the tricritical point, which is at $a=b=0$, the phase boundary is described by the power law (5) with ψ

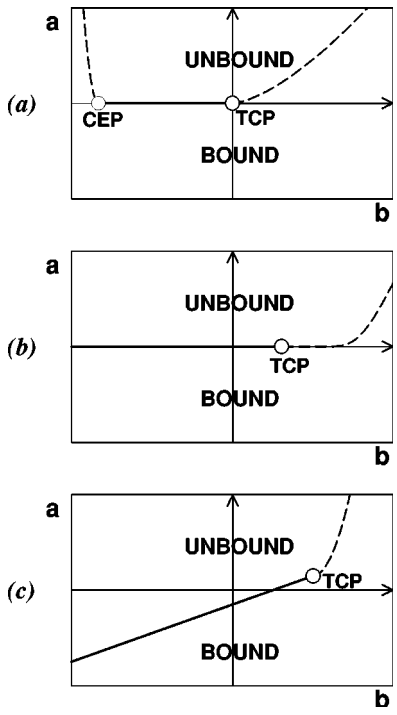

FIG. 3. Schematic representation of the renormalized (a-b) phase diagram obtained from the Fisher-Jin model (8) for the different fluctuation regimes. Critical wetting phase boundaries are shown by thick solid lines and first-order phase boundaries by dashed lines. (a) corresponds to all regimes with $\omega<1/2$, (b) corresponds to $1/2<\omega<2$, while (c) represents the case $\omega>2$.

$=(2-3\omega)/(1-3\omega)$. On the other hand, the asymptotic behavior of this phase boundary for large b reads

$$a\sim e^{-[(1-\omega)/(1-2\omega)][(1+\omega)/(\omega)]}(b\omega)^{(2-3\omega)/2(1-2\omega)}, \tag{17}$$

which incorporates the result (12) when ω is very small. Note this behavior is quantitatively different from that found from the capillary wave model where $a\sim b^{(2-3\omega)/(1-3\omega)}$ for all b. As in the mean-field approach discussed above, we find an additional first-order phase boundary which starts at a critical end point located at

$$|b_{\mathrm{CEP}}|=\frac{c^{2(1-2\omega)/(2-3\omega)}}{\omega}e^{-[(2-6\omega)/(2-3\omega)][(1-\omega)/\omega]}. \tag{18}$$

This result, which for small ω recovers Eq. (13), predicts that $|b_{\mathrm{CEP}}|$ increases upon increasing ω, and thus the window of critical transitions grows. Once again the presence of this critical end point has no physical meaning and its location diverges to $-\infty$ in the limit of $c\to\infty$.

When $4\omega t<l<6\omega t$ both the soft-wall restriction and the last exponential in Eq. (2) contribute Gaussians to the renormalized binding potential and so we consider

$$W^{(t)}(l)\approx ae^{-l+(2+\omega)t}+b[1-\omega(l-4\omega t)]e^{-2l+(2+4\omega)t}+\frac{D}{\sqrt{t}}e^{2t-l^2/4\omega t}, \tag{19}$$

where D is a positive constant. We find that this regime is valid for $2/9<\omega<1/2$ and that the phase diagram is qualitatively identical to the result of the previous regime, i.e., the phase diagram shown in Fig. 3(a). Quantitatively, some minor changes are predicted. For example, near the tricritical point, which remains at the origin, the first-order phase boundary behaves again as $a\sim b^{\psi}$ with in this case $\psi=(\sqrt{2}-\sqrt{\omega})^2/(\sqrt{2}-2\sqrt{\omega})^2$, while for large b the result (17) still applies. We further observe that the minimum at finite l near the critical end point tends to a boundary minimum for which the standard matching technique of the RG analysis is not suitable. From Eq. (18) and the predictions in the next regime (see below) we anticipate, however, that the critical end point diverges to $-\infty$ when $\omega\to 1/2-$, thereby completely removing this unphysical artifact.

A third regime is given by $2\omega t<l<4\omega t$ which is found to correspond to $1/2<\omega<2$. In this case the renormalized potential is given by

$$W^{(t)}(l)\approx ae^{-l+(2+\omega)t}+\frac{D(l/2\omega t)}{\sqrt{4\pi\omega t}}e^{2t-l^2/4\omega t}, \tag{20}$$

where

$$D(x)=\frac{w_0}{x}+\frac{b}{2-x}\left(1-\frac{\omega}{2-x}\right)+\frac{c}{3-x}. \tag{21}$$

Interestingly, the potential is identical in form to the one found for the capillary wave model in the corresponding regime, with only a small modification in the definition of $D(x)$ [5]. As a consequence, we find a phase diagram that is qualitatively the same as the one obtained without the position-dependent stiffness coefficient; however, the two phase diagrams are mirror images of one another, as can be seen from comparing Figs. 1(b) and 3(b). We discuss this result further in the next section. We additionally note that the tricritical point is shifted to $b_t>0$. The location of this point may be determined by setting $a=0$ in Eq. (20) and looking for a solution of $W=0$ for finite l. This yields

$$b_t(\omega)=\frac{(2-\sqrt{2/\omega})^2}{\omega+\sqrt{2/\omega}-2}\left[w_0\sqrt{\omega/2}+\frac{c}{3-\sqrt{2/\omega}}\right]. \tag{22}$$

For the critical and tricritical behavior we again recover the earlier predictions given in Eqs. (4) and (7), while the first-order boundary near the tricritical point follows an exponential path, just as in the case of the capillary wave model.

For the fourth regime, which applies for $\omega>2$, similar observations are found, resulting in a phase diagram that is topologically the same as in the standard model. In particular, at leading order all critical behavior and phase boundaries are identical to those found from the capillary wave model provided one incorporates the inversion $b\to -b$.

Our final comments in this section relate to the locus of tricritical behavior. This can typically be found from comparing the magnitude of the appropriate terms in the renormalized potential [5,13]. In so doing, we deduce that the predictions from the capillary wave model are not affected by the inclusion of a position-dependent stiffness coefficient. As a result, the region in which tricritical behavior is expected to be observed remains as represented by the dotted lines in Fig. 1, provided we again allow for the inversion $b \rightarrow -b$.

IV. DISCUSSION AND CONCLUSIONS

In this paper we have determined the full (a-b) phase diagram for the Fisher-Jin interface model, and compared these results with the corresponding ones from a traditional capillary wave model. The purpose of this analysis is to answer the question posed in the title: ''Is a position-dependent stiffness relevant for the wetting phase diagram?'' A direct comparison of the two phase diagrams (Fig. 1 and Fig. 3) certainly suggests a large change in the phase behavior. However, we argue that qualitatively the phase behavior is the same in the two cases so that for practical purposes the answer to the question is ''no.''

More specifically, the main effect of the position-dependent stiffness contribution is to reverse the sign of the next-to-leading order term in the appropriate binding potential. As a consequence the phase diagram is inverted with $b \rightarrow -b$. Bearing this in mind the two figures are essentially the same with differences in the $\omega < 1/2$ regimes (the critical end point and additional first-order phase boundary) simply being artifacts of truncating the binding potential as discussed in Sec. III. These observations are particularly relevant if one wishes to compare the phase diagrams with those found in experimental systems. For example, recent experimental observations of critical and first-order wetting in alkane-methanol mixtures are believed to be in the universality class of short-range wetting [16]. For long-chain alkanes first-order wetting is found while for shorter-chain alkanes a critical wetting transition has been reported. Thus we may tentatively identify a with the temperature and b with the alkane chain length (with the sign changing as the length is decreased); however, it makes no difference which of the two theoretical phase diagrams one compares with since their topology and the associated critical behaviors are identical. The only decision is whether to identify long chain lengths with positive or negative b. This freedom of choice is available because b is essentially a phenomenological parameter within the effective Hamiltonian theory. In practice we might hope to deduce the sign of b for a given chain length on physical grounds starting from a more microscopic theory and integrating out degrees of freedom. If this is possible the results presented in this paper would provide a mechanism for determining whether the capillary wave or FJ model has the stronger physical basis. For example, for the situation described above, if $b > 0$ for long-chain alkanes then the FJ model is preferred, whereas if $b < 0$ for long-chain alkanes then the capillary wave model would appear to be the better one. However, we are wary of attempting to make such a prediction at this stage since there is strong evidence that the reported wetting transitions will reveal only MF-like behavior (where the two theories are identical) due to the inability to perform experiments sufficiently close to the wetting temperature [16]. Thus at present we feel caution should be exercised in comparing the theory with experiments, but hope further progress can be made in this area in the near future.

Returning to the comparison of the two theories we comment that, at a quantitative level, there are some differences between the two phase diagrams for the interface models studied; however, these are apparent only for $\omega < 1/2$. Most notably the form of the first-order phase boundary away from the tricritical point is different in the two cases. Thus, for example in the limit of $\omega \rightarrow 0+$ the phase boundary is quadratic for the capillary wave model but linear for the Fisher-Jin model. Hence at this level we can argue that the position-dependent stiffness *is* relevant for the wetting phase diagram.

One final issue that we wish to address is the effect of fluctuations upon the phase diagrams. The original FJ analysis predicted a stiffness instability mechanism with critical wetting transitions being driven fluctuation induced first order [4]. However, we have argued that in contrast fluctuations tend to drive the first-order wetting transition second order. For example comparison of Figs. 3(a) and 3(b) shows such a change related to the shifting of the tricritical point as ω is increased. This is in complete accord with our findings from the capillary wave model discussed in Sec. II A. Thus one may ask where is the stiffness instability mechanism is in our results. The answer is that FJ considered only the region of the phase diagram with $b > 0$, and compared the simple mean-field phase diagram in the absence of the stiffness contribution [Fig. 2(a)] with the renormalized phase diagram given in Fig. 3. Under such a comparison one indeed sees the critical wetting transition being largely replaced by a first-order transition. However, this transformation occurs immediately one allows the stiffness term to contribute (i.e., as one goes from $\omega = 0$ to $\omega = 0+$) and as such is not really a fluctuation effect.

In conclusion we summarize our main results. The effect of including a position-dependent stiffness coefficient is made up of two distinct contributions. First, upon noting that the coefficient of this term is proportional to the next-to-leading order term in the bare binding potential, but opposite in sign, one finds a discontinuous change in the phase diagram immediately upon moving beyond the MF level. This discontinuity is simply an inversion of the phase diagram. Secondly, the presence of fluctuations tends to drive the first-order wetting transition critical. Finally, for practical purposes we note that the qualitative features of the phase diagram are completely unaffected by the inclusion of the stiffness contribution, as are recent predictions for tricritical wetting [5].

ACKNOWLEDGMENTS

We would like to thank Joseph Indekeu for helpful discussions over a number of years. This research was supported by the EPSRC, UK (GR/N37070) and the Nuffield Foundation (NUF-NAL 99).

[1] For a general review of wetting, see S. Dietrich, in *Phase Transitions and Critical Phenomena*, Vol. 12, edited by C. Domb and J. L. Lebowitz (Academic, London, 1988).
[2] A review of RG methods applied to interface behavior is given by G. Forgacs, R. Lipowsky, and Th. M. Nieuwenhuizen, in *Phase Transitions and Critical Phenomena*, edited by C. Domb and J. L. Lebowitz (Academic, London, 1991), Vol. 14.
[3] Recent advances in wetting in systems with short-range forces are reviewed by C. J. Boulter, Mod. Phys. Lett. B **15**, 993 (2001).
[4] M. E. Fisher and A. J. Jin, Phys. Rev. Lett. **69**, 792 (1992).
[5] C. J. Boulter and F. Clarysse, Eur. Phys. J. E **5**, 465 (2001).
[6] R. Lipowsky, D. M. Kroll, and R. K. P. Zia, Phys. Rev. B **27**, 4499 (1983).
[7] E. Brézin, B. I. Halperin, and S. Leibler, Phys. Rev. Lett. **50**, 1387 (1983).
[8] D. S. Fisher and D. A. Huse, Phys. Rev. B **32**, 247 (1985).
[9] R. Lipowsky, J. Phys. A **18**, L585 (1985); R. Lipowsky and T. M. Nieuwenhuizen, *ibid.* **21**, L89 (1988).
[10] E. H. Hauge and K. Olaussen, Phys. Rev. B **32**, 4766 (1985).
[11] K. Binder and D. P. Landau, Phys. Rev. B **37**, 1745 (1988).
[12] A. J. Jin and M. E. Fisher, Phys. Rev. B **47**, 7365 (1993).
[13] A. J. Jin and M. E. Fisher, Phys. Rev. B **48**, 2642 (1993).
[14] Monte Carlo simulations of a lattice version of the interface model suggest that the soft-wall approximation has no significant effect on the results since both hard- and soft-wall restrictions yield the same critical behavior; see G. Gompper and D. M. Kroll, Europhys. Lett. **5**, 49 (1988); Phys. Rev. B **37**, 3821 (1988).
[15] R. Evans, D. C. Hoyle, and A. O. Parry, Phys. Rev. A **45**, 3823 (1992).
[16] D. Ross, D. Bonn, and J. Meunier, Nature (London) **400**, 737 (1999); J. Chem. Phys. **114**, 2784 (2001).